Submitted to Journal of Electroanalytical Chemistry

LBL-6018
Preprint c. 1

SIMULTANEOUS REACTIONS ON A ROTATING-DISK ELECTRODE

Ralph White and John Newman

January 1977

Prepared for the U. S. Energy Research and Development Administration under Contract W-7405-ENG-48

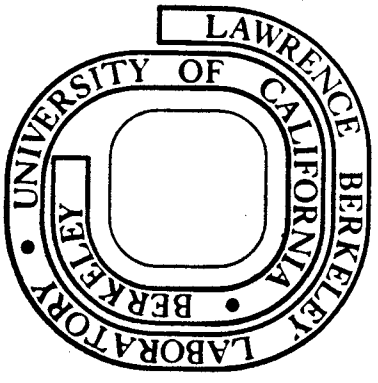

LBL-6018
c. 1

DISCLAIMER

LBL-6018

Simultaneous Reactions on a Rotating-Disk Electrode

Ralph White and John Newman

Materials and Molecular Research Division, Lawrence Berkeley Laboratory
and Department of Chemical Engineering, University of California,
Berkeley, California 94720

January, 1977

Abstract

Multiple reactions at a rotating-disk electrode are modeled. The governing equations are used to generate a parameter which characterizes the effect of a side reaction on the limiting-current curve of a main reaction. Various predicted current-potential curves illustrate the importance of this parameter for copper deposition with simultaneous formation of dissolved hydrogen at a disk electrode rotating in a copper sulfate solution containing sulfuric acid.

Distributions of current, potential, and surface concentration on the disk indicate that in some cases the main reaction can be below its limiting rate at the center of the disk while hydrogen gas bubbles may be formed near the edge. In addition, predicted and measured limiting-current curves for this system are compared.

Introduction

The rotating-disk electrode is a popular experimental tool.[1-6] It has been used, for example, to measure diffusion coefficients, investigate metal deposition and organic synthesis, determine bulk concentrations of electroactive species, and study corrosion. Multiple electrode reactions occur invariably to some extent in all of these cases. To help understand better their effect, a model of an electrochemical cell consisting of a rotating-disk electrode on which multiple reactions can occur, a distant counterelectrode, and a reference electrode of a given kind is presented.

White et al.[7] presented a similar model which included multiple electrode reactions and the effect of ionic migration but neglected the nonuniformity of the ohmic potential drop in solution. The present model includes this effect but neglects that due to ionic migration within the diffusion layer.

The model is similar to ones presented earlier.[8-28]

Model

Assumptions

The following assumptions apply to the model:

1. There are two types of species: major and minor. The major species are the dissociation products of the supporting electrolyte; all other species are minor. The concentration of supporting electrolyte is constant. Minor species are transported according to the theory of transport processes in infinitely dilute electrolytic solutions.[22]

Diffusion coefficients and other physical properties of the solution depend only on the bulk composition.

2. The diffusion potential difference across the diffusion layer is negligible. Also, the potential in a separate reference-electrode compartment is assumed to be the same as that in the bulk solution at the entrance to the connecting capillary tube.

3. The local current density just outside the diffuse double layer on the rotating-disk electrode is the same as that at the outer edge of the diffusion layer.

4. The surface of the disk remains uniformly smooth during metal deposition.

5. The system is isothermal and operated at steady state, so that charging currents are negligible.

6. The Schmidt number of each minor species is large.

Bulk solution

The potential distribution in the solution outside the diffusion layer is governed by Laplace's equation. For the disk geometry, the general solution satisfying the condition of an insulating plane surrounding a disk electrode of radius r_o and remaining finite on the axis of the disk, can be expressed as[10,21]

$$\tilde{\Phi}(\eta,\xi) = \sum_{n=0}^{\infty} B_n P_{2n}(\eta) M_{2n}(\xi) \quad , \tag{1}$$

where η and ξ are rotational elliptic coordinates, natural to the disk geometry, and are related to cylindrical coordinates r and z by the relationships

$$z = r_o \xi \eta \tag{2}$$

and

$$r = r_o[(1 + \xi^2)(1 - \eta^2)]^{1/2} \ . \tag{3}$$

$P_{2n}(\eta)$ is the Legendre polynomial of order $2n$, and $M_{2n}(\xi)$ is a corresponding Legendre function of imaginary argument[10,29] normalized in such a way that $M_{2n} = 1$ at $\xi = 0$. The potential distribution in equation 1 also approaches zero as ξ approaches infinity, corresponding to a distant placement of the counterelectrode.

Diffusion layer

When the effect of ionic migration is ignored, the concentrations of minor species are found to satisfy the equation of convective diffusion. For the high values of the Schmidt number ν/D_i commonly enountered in electrolytic solutions, the velocity profiles can be approximated by their forms close to the disk surface, and this equation can be solved even though the concentration of a species is not constant along the surface. The resulting normal component of the flux density at the surface can be expressed as an integral over this variation of the surface concentration:[11,30,31]

$$N_i(r) = -D_i \left.\frac{\partial c_i}{\partial z}\right|_{z=0} = \frac{-(D_i^2 D_R)^{1/3}}{\delta_d \Gamma(4/3)} \left[c_{i,\infty} - c_{i,o}(0) - r \int_o^r \frac{dc_{i,o}(x)}{dx} \frac{dx}{(r^3 - x^3)^{1/3}} \right] , \tag{4}$$

where δ_d is the diffusion-layer thickness,

$$\delta_d = \left(\frac{3D_R}{a\nu}\right)^{1/3} \left(\frac{\nu}{\Omega}\right)^{1/2} , \tag{5}$$

based on the diffusion coefficient D_R of the principal reactant, the rotation speed Ω, and the kinematic viscosity ν of the fluid.

Current densities and multiple reactions

An electrochemical reaction j can be written abstractly as

$$\sum_i s_{ij} M_i^{z_i} \rightarrow n_j e^- , \tag{6}$$

where n_j denotes the number of electrons transferred and M_i represents species i, z_i its charge number, and s_{ij} its stoichiometric coefficient. Let the rate of each possible reaction be represented by the value i_j of its contribution to the total (local) electrode current density i_T. Then the flux densities of solution species at the electrode surface are given in the steady state by Faraday's law:

$$N_i(r) = - \sum_j \frac{s_{ij} i_j}{n_j F} . \tag{7}$$

It has furthermore been assumed that the diffusion layer is so thin that the total current density can be obtained either from the sum of partial current densities for the electrode reactions or from the derivative of the potential distribution (equation 1) prevailing outside the diffusion layer:

$$i_T(r) = \sum_j i_j = -\kappa_\infty \left.\frac{\partial \tilde{\Phi}}{\partial z}\right|_{z=0} , \qquad (8)$$

where κ_∞ is the conductivity of the bulk solution. The orthogonality of the Legendre polynomials and the values[10,21] of $M'_{2n}(0)$ permit the coefficient B_n in equation 1 to be expressed as an integral over the electrode current density i_T :

$$B_n = [P_{2n}(0)]^2 \frac{(4n+1)\pi r_o}{2\kappa_\infty} \int_0^1 \eta i_T P_{2n}(\eta) d\eta . \qquad (9)$$

The local current density due to reaction j is related to the surface overpotential for reaction j and the surface concentrations of the species by the Butler-Volmer equation

$$i_j = i_{oj,ref} \prod_i \left(\frac{c_{i,o}}{c_{i,ref}}\right)^{\gamma_{ij}} \left[\exp\left(\frac{\alpha_{aj} F}{RT} \eta_{sj}\right) - \exp\left(-\frac{\alpha_{cj} F}{RT} \eta_{sj}\right)\right] , \qquad (10)$$

where $c_{i,ref}$ is a reference concentration, $i_{oj,ref}$ is a value of the exchange current density for reaction j calculated at the composition $c_{i,ref}$, and γ_{ij} is an exponent expressing the composition dependence of the exchange current density.

The surface overpotential η_{sj} for reaction j can be expressed as

$$\eta_{sj} = V - \Phi_o - U_{j,o} , \qquad (11)$$

that is, it is the difference between the electrode potential V and

the potential $\Phi_o(r)$ in the solution just outside the diffuse part of the double layer, minus the theoretical open-circuit potential $U_{j,o}$ for reaction j. Both Φ_o and $U_{j,o}$ are measured by a reference electrode of a given kind, corrected for any liquid-junction potential which might exist between the solution in question and that within the reference-electrode compartment (see section 40 of reference 22). $U_{j,o}(r)$ is related to the local solution composition as well as the nature of the reference electrode. In the dilute-solution approximation used here, activity-coefficient corrections can be ignored, and this relationship becomes

$$U_{j,o} = U_j^\theta - U_{re}^\theta - \frac{RT}{n_j F} \sum_i s_{ij} \ln\left(\frac{c_{i,o}}{\rho_o}\right) + \frac{RT}{n_{re} F} \sum_i s_{i,re} \ln\left(\frac{c_{i,re}}{\rho_o}\right) . \quad (12)$$

If the usual tabulations of standard electrode potentials are used for U_j^θ and U_{re}^θ, the concentrations in equation 12 must be expressed in moles/liter. Alternatively, the pure solvent density ρ_o can be expressed in kg/cm^3 instead of g/cm^3.

If we set ξ equal to zero in equation 1, we obtain $\tilde{\Phi}_o$, the potential in the bulk solution extrapolated to the electrode surface as if the current distribution was unchanged but there were no concentration variation in the diffusion layer. With the supporting-electrolyte approximation used here, Φ_o in equation 11 is indistinguishable from $\tilde{\Phi}_o$ because any diffusion potential and any conductivity variation across the diffusion layer are neglected.

Parameters

It is frequently useful to introduce a dimensionless formulation of the problem because in this manner it is possible to identify a small number of dimensionless parameters which govern a system. These may specify laws of similitude which show how the system depends on size or rotation speed, and in favorable situations it may be possible to compute general solutions which apply to a number of different chemical systems over a range of compositions and temperatures. These are very useful for instruction, scale-up, and for drawing general conclusions about system behavior.

However, the reduction in the number of parameters is limited for complex systems where there are several relevant species in solution and several possible electrode reactions. For example, if the potentials, including overpotentials and open-circuit potentials, are made dimensionless with RT/F, there remain as dimensionless parameters the transfer coefficients of the electrode reactions. Even if one recognizes that cathodic processes with a main reaction m are most important and makes the potentials dimensionless with $RT/\alpha_{cm}F$, there remain the ratios of the transfer coefficients to α_{cm}. Furthermore, there are the exponents γ_{ij} and the ratio of the stoichiometric coefficients s_{ij} to n_j. For the minor species, there are the bulk composition, the reference concentrations $c_{i,ref}$, and the ratios D_i/D_R of diffusion coefficients to that of the principal reactant. (One cannot generally set $c_{i,ref}$ equal to $c_{i,\infty}$ because some species may not be present in the bulk solution.) These considerations suggest that we must deal with specific chemical systems or a narrow class of systems.

Nevertheless, even for specific systems it will be instructive to introduce parameters related to the size and the rotation speed. When we are concerned with the effects of a nonuniform ohmic potential drop in the solution, current densities should be made dimensionless with $RT\kappa_\infty/Fr_o$, or with $|s_{Rm}/n_m|\ RT\kappa_\infty/Fr_o$ to be consistent with previous work.[10] The dimensionless average current density is then

$$\delta = \frac{-n_m Fr_o}{s_{Rm} RT\kappa_\infty} i_{avg} , \tag{13}$$

and dimensionless exchange current densities are

$$J_j = -\frac{n_m}{s_{Rm}} \frac{Fr_o}{RT\kappa_\infty} i_{oj,ref} . \tag{14}$$

According to the Levich equation,[32] the limiting current density for the principal reactant is

$$i_{m,lim} = \frac{n_m F D_R c_{R,\infty}}{s_{Rm} \Gamma(4/3) \delta_d} . \tag{15}$$

This leads to the dimensionless limiting-current density*

$$N = \Gamma(4/3) \frac{n_m Fr_o}{s_{Rm} RT\kappa_\infty} i_{m,lim} = \frac{n_m^2 F^2 D_R c_{R,\infty}}{s_{Rm}^2 RT\kappa_\infty} \left(\frac{a\nu}{3D_R}\right)^{1/3} \left(\frac{r_o^2 \Omega}{\nu}\right)^{1/2} , \tag{16}$$

which can also be thought of as a dimensionless (square root of) rotation speed.

*To be consistent with earlier work,[10] $\Gamma(4/3)$ is inserted as shown.

Let us also identify a single parameter which will characterize the manner in which a side reaction tends to obscure the limiting-current plateau for a main, or desired, reaction. It is the magnitude of the side reaction relative to the main reaction at potentials in the neighborhood of the limiting-current plateau which is important (see figure 1). At these potentials, it is unlikely that the backward terms in the Butler-Volmer equation 10 have a major influence, and a Tafel approximation could be applied for both the main and side reactions. For our example, the cathodic processes are involved.

The electrode potential V_m for which the main reaction is beginning to reach the limiting current is, in the absence of an ohmic potential drop, approximately equal to

$$V_m = U_{m,ref} - \frac{RT}{\alpha_{cm}F} \ln \left| \frac{i_{m,lim}}{i_{om,ref}} \right| , \qquad (17)$$

where $U_{m,ref}$ is given by equation 12 but with reference concentrations in place of the surface concentrations. At this potential defined by equation 17, the current density for the side reaction j divided by the limiting current density for the main reaction (see equation 15) is proportional to $\exp(-\alpha_{cj}F\Delta U_j/RT)$, where

$$\Delta U_j = U_{m,ref} - U_{j,ref} - \frac{RT}{\alpha_{cj}F} \ln \left| \frac{i_{oj,ref}}{i_{m,lim}} \right| + \frac{RT}{\alpha_{cm}F} \ln \left| \frac{i_{om,ref}}{i_{m,lim}} \right| . \qquad (18)$$

This parameter makes it clear that it is neither the exchange current density nor the open-circuit potential alone which determines the

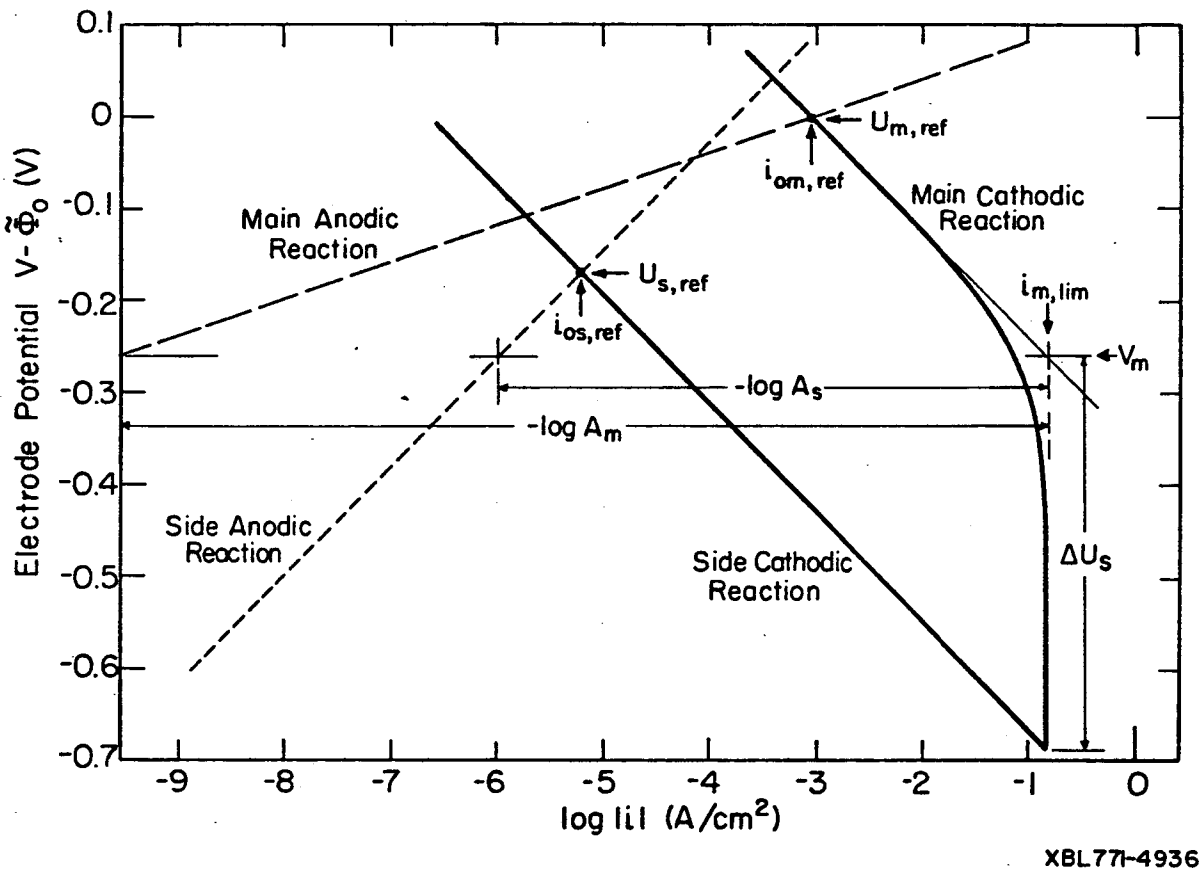

Figure 1. Qualitative sketch of the current-potential curves for a main and a side reaction showing some of the parameters defined in the text.

relative significance of a side reaction. If either the exchange current density is very small or the open-circuit potential is quite negative, the side reaction will not obscure the limiting-current plateau.

In the case of a corrosion process, a different selection of parameters would be appropriate, one placing emphasis on the anodic part of one reaction and the cathodic part of another reaction.

If equations 7, 10, and 11 are substituted into equation 4 and use is made of the definitions in equations 12, 15, 17, and 18, one obtains the equation (one for each minor species i)

$$\frac{s_{Rm}}{n_m}\frac{(D_i/D_R)^{2/3}}{c_{R\infty}}\left[c_{i,\infty} - c_{i,o}(0) - r\int_o^r \frac{dc_{i,o}}{dx}\frac{dx}{(r^3-x^3)^{1/3}}\right]$$

$$= \sum_j \frac{s_{ij}}{n_j}\exp\left(-\frac{\alpha_{cj}F}{RT}\Delta U_j\right)\exp\left[-\frac{\alpha_{cj}F}{RT}(V - V_m - \tilde{\Phi}_o)\right]\prod_k\left(\frac{c_{k,o}}{c_{k,ref}}\right)^{q_{kj}}$$

$$- \sum_j \frac{s_{ij}}{n_j}A_j\exp\left[\frac{\alpha_{aj}F}{RT}(V - V_m - \tilde{\Phi}_o)\right]\prod_k\left(\frac{c_{k,o}}{c_{k,ref}}\right)^{p_{kj}}, \qquad (19)$$

where the cathodic and anodic reaction orders are

$$q_{kj} = \gamma_{kj} - \alpha_{cj}\frac{s_{kj}}{n_j} \quad \text{and} \quad p_{kj} = \gamma_{kj} + \alpha_{aj}\frac{s_{kj}}{n_j} \qquad (20)$$

and the parameter

$$A_j = \left|\frac{i_{oj,ref}}{i_{m,lim}}\right|^{1+\alpha_{aj}/\alpha_{cj}}\exp\left(\frac{\alpha_{aj}F}{RT}\Delta U_j\right) \qquad (21)$$

characterizes the magnitude of the anodic part of reaction j at an electrode potential related to the limiting-current plateau for the main reaction. The influence of the parameter A_m for a main reaction alone on the shape of limiting-current curves was investigated in 1955 by Gerischer[33] (see also references 5 and 34).

Solution Technique

As in earlier work,[12] one alternates between revising the surface concentrations and improving the potential distribution, iterating between the two until no further improvement is noticed.

For a given distribution of $V - \tilde{\Phi}_o$, equation 19 (one for each minor species i) governs the surface concentration distributions $c_{i,o}$. For calculational convenience, we specify $c_{R,o}$ at the center of the disk. Equation 19 is solved by a multidimensional Newton-Raphson iteration method for the value of $V - \tilde{\Phi}_o$ and the other values of $c_{i,o}$ at the center of the disk. As a start, it is assumed that this potential difference applies across the whole surface of the electrode.

More generally, with the best possible radial distribution of $V - \tilde{\Phi}_o$, equation 19 is solved for the surface concentration distributions by a generalization of the technique of Acrivos and Chambré.[35] This involves evaluation of the integrals by means of discrete mesh points evenly spaced in r^3. One proceeds from the center of the electrode toward its edge, and at each mesh point he solves the coupled equations 19 by the multidimensional Newton-Raphson method. This procedure gives implicitly the distribution of current density for each reaction j and hence for the total current density i_T.

From the current-density distribution determined above, one next calculates a new distribution of potential $\tilde{\Phi}_o$ from equation 1 after first calculating a finite number of values of B_n by means of equation 9. (A damping technique, whereby $\tilde{\Phi}_o$ values are averaged with previously estimated values, can be used here to speed overall convergence.) The value of V is adjusted so that $V - \tilde{\Phi}_o$ at the center of the disk is the same as that originally calculated.

The procedure in the last two paragraphs is repeated until a convergence criterion is satisfied.

Results and Discussion

The utility of the model is demonstrated by the simulation of copper deposition

$$Cu^{++} + 2e^- \rightarrow Cu \ , \tag{22}$$

as the main reaction and the formation of dissolved hydrogen

$$H^+ + e^- \rightarrow \frac{1}{2} H_2 \ , \tag{23}$$

as the side reaction. Table 1 gives parameters for these processes in a cupric sulfate solution containing sulfuric acid, where the kinematic viscosity* is $\nu = 0.010795$ cm^2/s and the bulk conductivity** is $\kappa_\infty = 0.54373$ ohm^{-1} - cm^{-1} . The cathodic transfer coefficients were set equal to 0.5; the anodic transfer coefficients were set equal

*Average value for the polarograms shown in figure 2.[36]
**Determined from Hsueh's correlation.[37]

Table 1. Parameter values for copper deposition at 298.15 K. The exchange current densities and the diffusion coefficient of cupric ions were determined by fitting the model to the data. The reference concentration for H_2 corresponds to the solubility in water at one atmosphere partial pressure.

Species	$10^6 D_i$	$c_{i,\infty}$	$c_{i,ref}$	γ_{im}	γ_{is}
	cm^2/s	mol/l	mol/l		
Cu^{++}	7.5	5.81×10^{-3}	$c_{R,\infty}$	0.42[b]	0
H_2	38[a]	4.155×10^{-10}	8.31×10^{-4}	0	0.25
H^+	——	1.5[c]	1.5[c]	0	0.5

Reaction	U_j^θ	$i_{oj,ref}$
	V	A/cm^2
main	0.337	9.08×10^{-4}
side	0	6.124×10^{-6}

[a] Arbitrarily selected for this work. (See reference 38).

[b] Taken from reference 22 (see also reference 39).

[c] It is assumed here that the dissociation products of H_2SO_4 are H^+ and HSO_4^- and that the bisulfate ion does not dissociate.

to 1.5 and 0.5 for the main and side reactions, respectively.

Predicted and measured[40] current-potential curves for this system are shown in figure 2. The comparison was used to determine some of the parameters in table 1. For the choice of transfer coefficients used here, ΔU_s is independent of the rotation speed.

Figure 3 shows how the shape of the current-potential curves depends on N and ΔU_s, where the bulk concentration of the principal reactant and the supporting electrolyte concentration were set equal to 0.1 and 1.0 M, respectively. ΔU_s and N were varied by changing the exchange current density of the side reaction and the disk size, respectively. Hsueh's correlations[37] were used to determine the solution density, viscosity, conductivity, and the cupric ion diffusion coefficient as a function of the bulk concentration of $CuSO_4$ and H_2SO_4, and the rotation speed was set at 2500 rpm (261.8 rad/s). In this case, the anodic portion of the side reaction is negligible in the potential range shown, and the anodic portion of the main reaction is significant only near the open-circuit potential (an abscissa value of 0.19 V). The results are therefore applicable to other systems with similar values of the cathodic transfer coefficients and reaction orders, and they illustrate qualitatively the expected behavior for systems with different parameters.

In figure 4, the desired values of ΔU_s were obtained by varying the bulk concentration of the principal reactant, thereby increasing A_m, while holding $c_{H_2SO_4} = 1.0$ M. Where the anodic

portion of the main reaction is not negligible, figure 4 must be used; otherwise, for values of $V - \tilde{\Phi}_o(r = 0)$ more negative than about -0.025 V , the curves would agree with those of figure 3 if plotted against the same abscissa.

The maximum variation of the potential $\tilde{\Phi}_o$ in the solution across the surface of the disk occurs when the current density distribution is uniform (as, for example, at the limiting current for a single reaction) and then has the value[10,41]

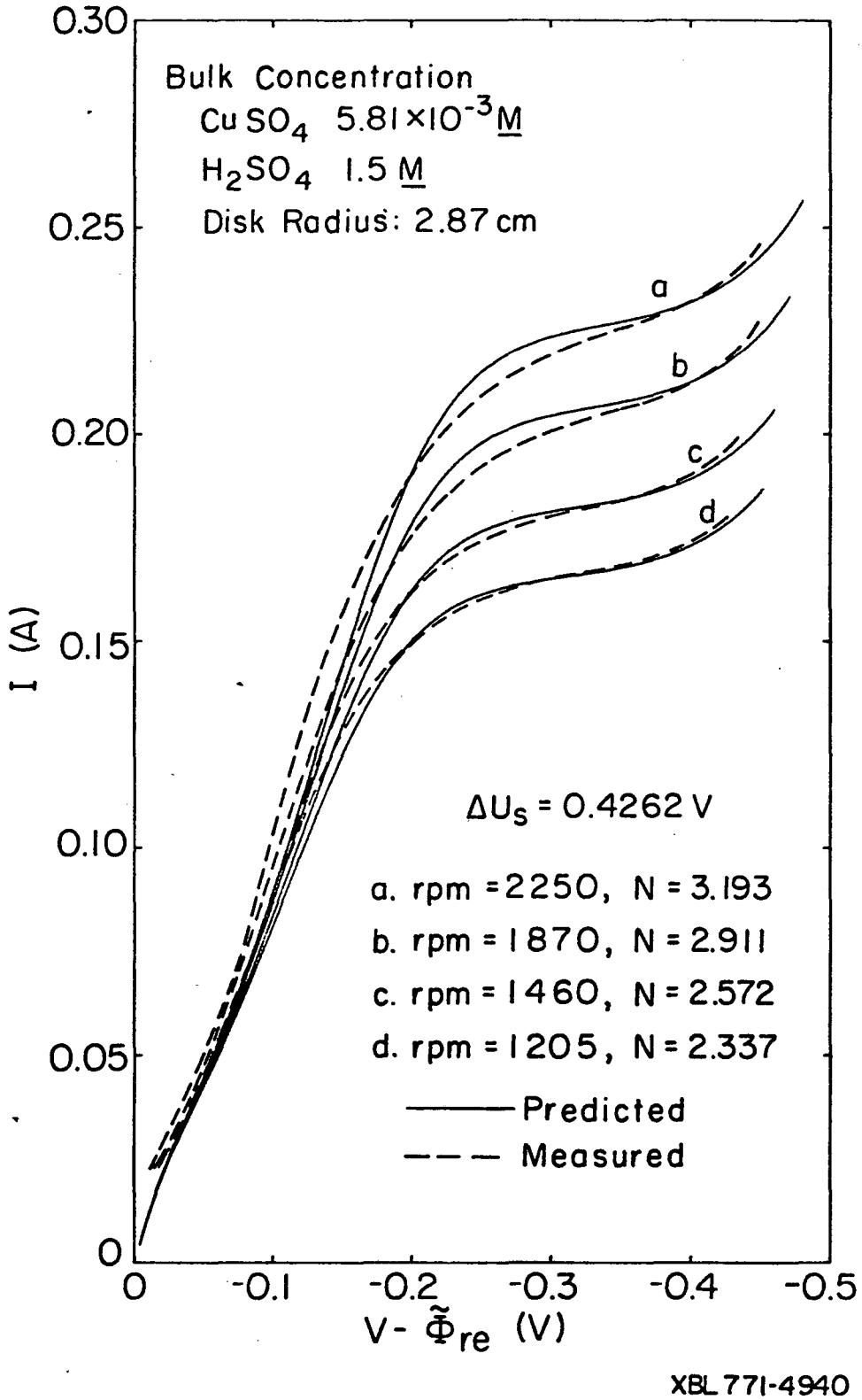

Figure 2. Comparison of predicted and measured[40] limiting current curves for copper deposition with simultaneous formation of dissolved hydrogen. The reference electrode was a copper wire located in the bulk solution; its position in the experimental cell was approximated in the model by placing it in the plane of the disk, 5 cm from the axis of rotation.

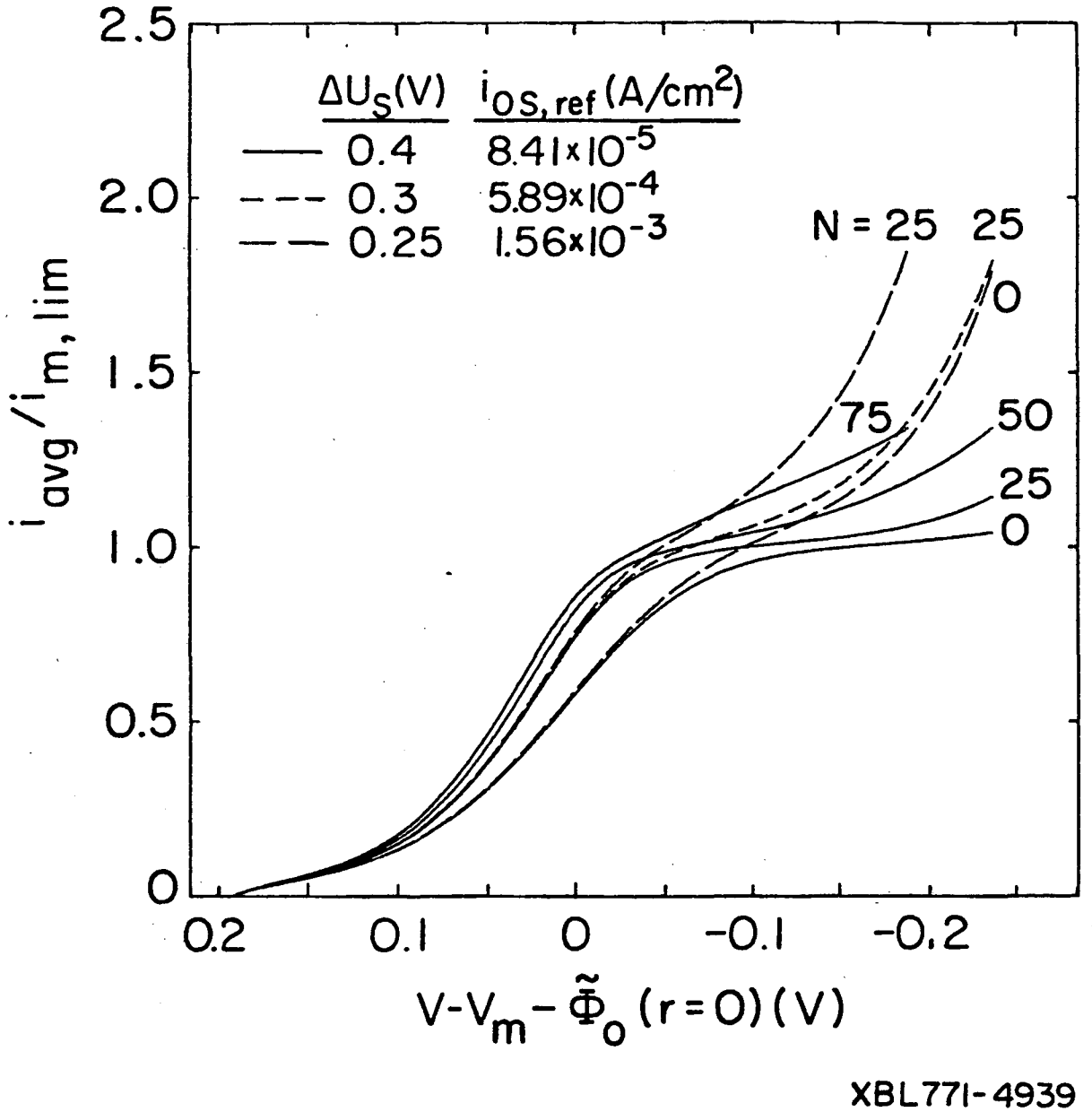

Figure 3. Simulated current-potential curves for copper deposition with simultaneous dissolved hydrogen formation, where the anodic portion of the side reaction is negligible and the anodic portion of the main reaction is significant only near the open-circuit potential. The reference exchange current density for the main reaction is $i_{om,ref} = 3\times10^{-3}$ A/cm^2 and $A_m = 3.52\times10^{-7}$.

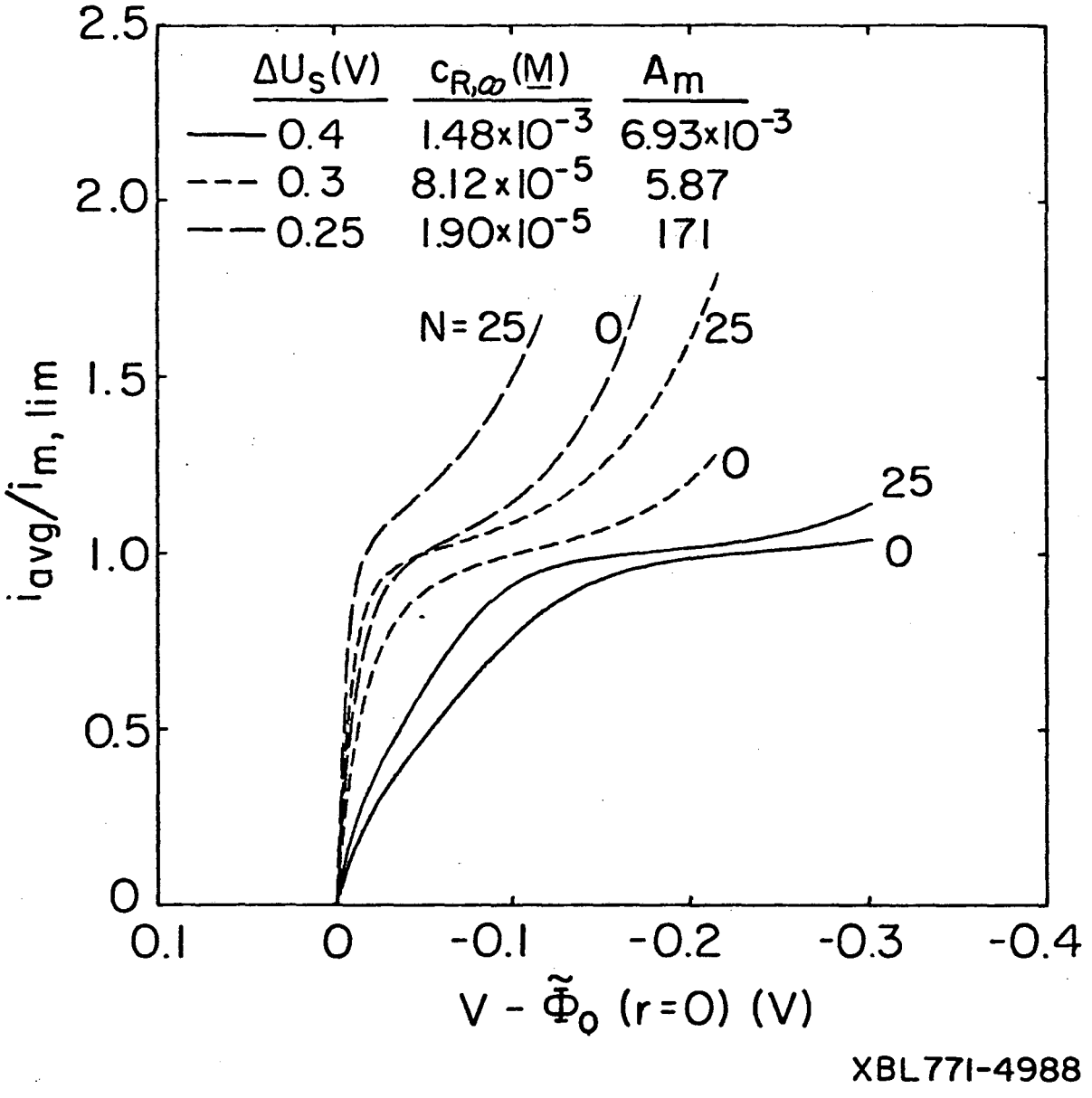

Figure 4. Simulated current-potential curves for copper deposition with simultaneous dissolved hydrogen formation, where the anodic portion of the side reaction is negligible. The reference exchange current density of the side reaction is $i_{os,ref} = 5\times10^{-6}$ A/cm^2.

$$\Delta\tilde{\Phi}_o = 0.363 \frac{r_o i_{avg}}{\kappa_\infty} . \qquad (24)$$

The current densities of interest here are approximately equal to $i_{m,lim}$. Thus, the parameter N provides a measure of the potential variation in the solution to be expected at the limiting current, expressed in units of RT/F .

Curves for N = 0 in figures 3 and 4 thus describe a situation where the disk is so small that the entire electrode is at a uniform potential relative to the adjacent solution. The shape of these curves shows how the side reaction occurs at the same potential as the main reaction and obscures the limiting-current plateau more as ΔU_s becomes smaller. Figure 2 also illustrates that distortion of the limiting-current plateau can occur even for a relatively small value of N and a large value of ΔU_s .

Since ΔU_s depends on the reference concentrations, they should be chosen appropriately (see table 1) to ensure that ΔU_s is characteristic of the physical system under study. For example, lowering the bulk concentration of the principal reactant to reduce N would also lower ΔU_s .

The value of A_m also influences the shape of current-potential curves, as discussed by Gerischer[33] in the abscence of a side reaction. Comparison of the curves for N = 0 on figure 4 shows that below the limiting current the importance of the anodic portion of the main reaction increases as A_m increases.

Distortion of the limiting-current plateau (see figure 3) becomes more pronounced as N increases for a given value of ΔU_s. (The disk sizes necessary to make $N = 25$ for the $c_{R,\infty}$ values shown in figure 4 are unrealistically large from an experimental standpoint.) As discussed above, for large N there can be an appreciable variation of $V - \tilde{\Phi}_o$ from the center to the edge of the electrode. The curve on figure 3 for $N = 50$ is expanded upon in figures 5 and 6. These figures show the radial distributions of current densities, surface

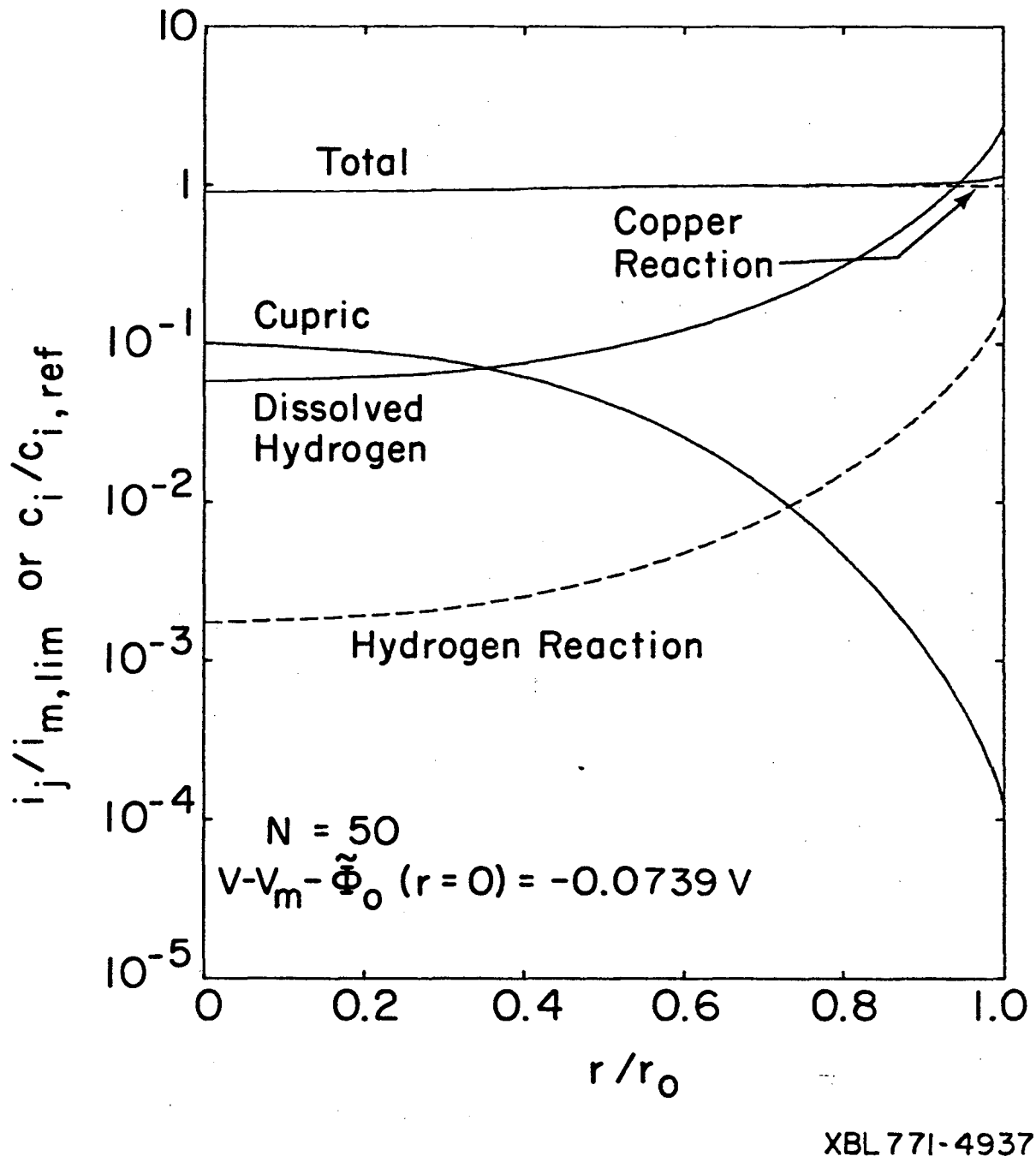

Figure 5. Radial current and surface concentration distributions. The reference concentration of the cupric species is the bulk value; that for hydrogen is the solubility. Hence, the solution is somewhat supersaturated in hydrogen toward the edge of the electrode.

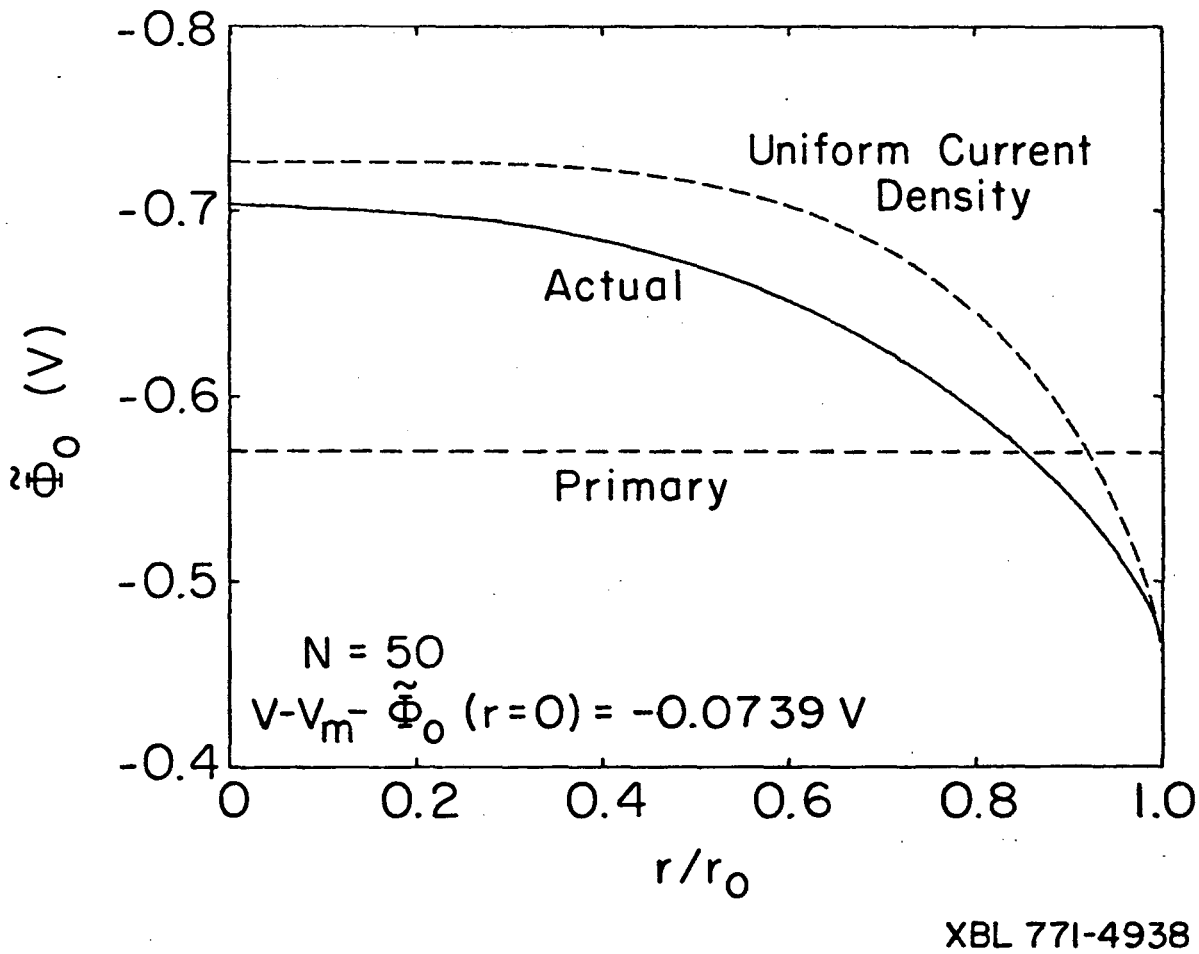

Figure 6. Radial potential distributions.

concentrations, and solution potential for a point well up on the limiting-current curve.

Figure 5 demonstrates that the main reaction current density can be below its limiting value at the center of the disk while hydrogen gas bubbles may be formed at the edge of the disk, since the dissolved hydrogen concentration exceeds its saturation value there by a factor of 2.388. However, larger supersaturation values of dissolved hydrogen with no bubble formation have sometimes been observed.[42]

The potential distribution labeled "Actual" in figure 6 gives rise to the nonuniform distributions in figure 5. The potential changes by about 0.236 V from the center to the edge of the disk because of its nonuniform accessibility from an ohmic standpoint. The potential labeled "Primary" was obtained from[43]

$$\tilde{\Phi}_o = I/4\kappa_\infty r_o \ .$$

The nonuniformity of the ohmic drop across the disk, as measured by N, can be an important cause of plateau distortion. On this basis, the distortion will be increased by increasing the rotation speed (or flow rates in general), disk size, or bulk concentration of the principal reactant. Some of these influences can be seen clearly in published sets of limiting-current curves. However, lowering $c_{R,\infty}$ can also lead to plateau distortion. This is the case because the magnitude of the main and side reactions approach one another as the bulk concentration of the principal reactant is lowered, as can be seen

by considering figure 1. The effect of $c_{R,\infty}$ is thus ambiguous -- a large value of $c_{R,\infty}/\kappa_\infty$ leads to distortion while a large value of $c_{R,\infty}/i_{os,ref}$ leads to a distinct plateau. For a reasonable value of $c_{R,\infty}$, the nonuniform ohmic effects can contribute significantly to plateau distortion for large disks or high rotation speeds. The competition of these several effects is adequately reflected in the definitions of the parameters N and ΔU_s and in the curves in figures 3 and 4 showing the resulting behavior.

Actually, with small disk electrodes and well supported solutions, plateau distortion is primarily due to the occurrence of the side reaction at the same potential as the main reaction (the ΔU_s effect). However, in technical applications where large systems become involved, one can be assured that the effect of nonuniform ohmic potential drop will be of great importance.

Summary

A model of the rotating-disk electrode with simultaneous reactions is presented. Predicted and measured current-potential curves are compared for copper deposition with simultaneous formation of dissolved hydrogen on a disk electrode rotating in a well-supported cupric sulfate solution.

Distortion of the limiting-current plateau for the main reaction by a side reaction can occur for two reasons. First, the side reaction can be in close proximity to the main reaction, as indicated by a small value of ΔU_s, and, second, a nonuniform ohmic potential drop, as

characterized by a large value of N, can promote the onset of a side reaction near the edge of the disk before the limiting-current condition is attained at the center.

Acknowledgement

This work was supported by the United States Energy Research and Development Administration.

Notation

a	0.51023262 (see reference 44)
A_j	parameter characterizing anodic reaction terms
B_n	coefficient in the expansion for the potential, V
c_i	concentration of species i, mol/cm^3
$c_{i,o}$	local surface concentration of species i
$c_{i,ref}$	reference concentration of species i
$c_{i,\infty}$	bulk concentration of species i
D_i	diffusion coefficient of species i, cm^2/s
F	Faraday's constant, 96,487 C/mol
i_{avg}	average current density, A/cm^2
i_j	local current density due to reaction j, A/cm^2
$i_{m,lim}$	limiting current density for the main reaction, A/cm^2
$i_{oj,ref}$	reference exchange current density, A/cm^2
i_T	total local electrode current density, A/cm^2
J_j	dimensionless exchange current density
M_i	symbol for the chemical formula of species i
M_{2n}	Legendre function of imaginary argument
n_j	number of electrons transferred in reaction j
N	dimensionless limiting current density
N_i	normal component of the flux density of species i, mol/cm^2-s

p_{ij}	anodic reaction order
P_{2n}	Legendre polynomial of order 2n
q_{ij}	cathodic reaction order
r	radial coordinate, cm
r_o	electrode radius, cm
R	universal gas constant, 8.3143 J/mol-K
s_{ij}	stoichiometric coefficient of species i in reaction j
T	absolute temperature, K
$U_{j,o}$	theoretical open-circuit potential for reaction j at the composition prevailing locally at the electrode surface, relative to a reference electrode of a given kind, V
$U_{j,ref}$	theoretical open-circuit potential evaluated for reference concentrations, V
U_j^θ	standard electrode potential for reaction j, V
ΔU_j	parameter characteristic of the cathodic part of reaction j relative to a main reaction, V
V	potential of the rotating-disk electrode, V
V_m	electrode potential characteristic of the limiting-current plateau for the main reaction, V
x	dummy integration variable, cm
z	axial coordinate, cm
z_i	charge number of species i
α_{aj}	anodic transfer coefficient for reaction j
α_{cj}	cathodic transfer coefficient for reaction j
γ_{ij}	exponent in composition dependence of exchange current density
$\Gamma(4/3)$	0.89298, the gamma function of 4/3
δ	dimensionless average current density
δ_d	diffusion-layer thickness, cm

η	rotational elliptic coordinate
η_{sj}	local surface overpotential for reaction j, V
κ_∞	bulk solution conductivity, $ohm^{-1} - cm^{-1}$
ν	kinematic viscosity of the solution, cm^2/s
ξ	rotational elliptic coordinate
ρ_o	pure solvent density, kg/cm^3
Φ_o	local solution potential adjacent to electrode surface, V
$\tilde{\Phi}$	potential in the solution outside the diffusion layer, V
$\tilde{\Phi}_o$	local potential in the bulk solution extrapolated to the electrode surface, V
Ω	rotation speed of the disk, rad/s

subscripts

o	at the electrode surface
m	main reaction
re	reference electrode
R	principal reactant
s	side reaction

References

1. A. C. Riddiford, "The Rotating Disk System," Advances in Electrochemistry and Electrochemical Engineering, 4 (1966), 47-116.

2. František Opekar and Přemysl Beran, "Rotating Disk Electrodes," Journal of Electroanalytical Chemistry, 69 (1976), 1-105.

3. V. Yu. Filinovsky and Yu. V. Pleskov, "Rotating Disk and Ring-Disk Electrodes in Investigations of Surface Phenomena at the Metal-Electrolyte Interface," Progress in Surface and Membrane Science, 10 (1976), 27-113.

4. W. J. Albery and M. L. Hitchman, Ring-disc Electrodes, London: Oxford University Press, 1971.

5. Jan Robert Selman, Measurement and Interpretation of Limiting Currents, Ph.D. Dissertation, University of California, Berkeley, 1971.

6. J. Robert Selman and Charles W. Tobias, "Mass-Transfer Measurements by the Limiting-Current Technique," Heinz Gerischer and Charles W. Tobias, eds., Advances in Electrochemistry and Electrochemical Engineering, 11, to be published.

7. Ralph White, James A. Trainham, John Newman, and Thomas W. Chapman, "Potential-Selective Deposition of Copper from Chloride Solutions Containing Iron," Journal of the Electrochemical Society, to be published.

8. Kameo Asada, Fumio Hine, Shiro Yoshizawa, and Shinzo Okada, "Mass Transfer and Current Distribution under Free Convection Conditions," Journal of the Electrochemical Society, 107 (1960), 242-246.

9. John Newman, "The Effect of Migration in Laminar Diffusion Layers," International Journal of Heat and Mass Transfer, 10 (1967), 983-997.

10. John Newman, "Current Distribution on a Rotating Disk below the Limiting Current," Journal of the Electrochemical Society, 113 (1966), 1235-1241.

11. John Newman, "The Diffusion Layer on a Rotating Disk Electrode," Journal of the Electrochemical Society, 114 (1967), 239.

12. W. R. Parrish and John Newman, "Current Distribution on a Plane Electrode below the Limiting Current," Journal of the Electrochemical Society, 116 (1969), 169-172.

13. D. H. Angell, T. Dickinson, and R. Greef, "The Potential Distribution near a Rotating-Disk Electrode," Electrochimica Acta, 13 (1968), 120-123.

14. W. J. Albery and J. Ulstrup, "The Current Distribution on a Rotating Disk Electrode," Electrochimica Acta, 13 (1968), 281-284.

15. Vinay Marathe and John Newman, "Current Distribution on a Rotating Disk Electrode," Journal of the Electrochemical Society, 116 (1969), 1704-1707.

16. Stanley Bruckenstein and Barry Miller, "An Experimental Study of Nonuniform Current Distribution at Rotating Disk Electrodes," Journal of the Electrochemical Society, 117 (1970), 1044-1048.

17. William H. Smyrl and John Newman, "Ring-Disk and Sectioned Disk Electrodes," Journal of the Electrochemical Society, 119 (1972), 212-219.

18. William H. Smyrl and John Newman, "Detection of Nonuniform Current Distribution on a Disk Electrode," Journal of the Electrochemical Society, 119 (1972), 208-212.

19. John Newman, "Engineering Design of Electrochemical Systems," Industrial and Engineering Chemistry, 60 (no. 4 , April, 1968), 12-27.

20. W. R. Parrish and John Newman, "Current Distributions on Plane, Parallel Electrodes in Channel Flow," Journal of the Electrochemical Society, 117 (1970), 43-48.

21. John Newman, "The Fundamental Principles of Current Distribution and Mass Transport in Electrochemical Cells," Allen J. Bard, ed., Electroanalytical Chemistry, 6 (1973), 187-352, New York: Marcel Dekker, Inc.

22. John S. Newman, Electrochemical Systems, Englewood Cliffs, N.J.: Prentice-Hall, Inc., 1973.

23. Peter Pierini, Peter Appel, and John Newman, "Current Distribution on a Disk Electrode for Redox Reactions," Journal of the Electrochemical Society, 123 (1976), 366-369.

24. Peter Pierini and John Newman, "Current Distribution on a Rotating Ring-Disk Electrode below the Limiting Current," Journal of the Electrochemical Society, to be published.

25. Richard Alkire and Ali Asghar Mirarefi, "The Current Distribution Within Tubular Electrodes under Laminar Flow," Journal of the Electrochemical Society, 120 (1973), 1507-1515.

26. Richard Alkire and Ali Asghar Mirarefi, "Current Distribution in a Tubular Electrode: Two Electrode Reactions," Journal of the Electrochemical Society, to be published.

27. Reinaldo Cabán and Thomas W. Chapman, "Rapid Computation of Current Distribution by Orthogonal Collocation," Journal of the Electrochemical Society, 123 (1976), 1036-1041.

28. Reinaldo Cabán and Thomas W. Chapman, "Statistical Analysis of Electrode Kinetics Measurements-Copper Deposition from $CuSO_4$-H_2SO_4 Solutions," Journal of the Electrochemical Society, to be published.

29. Philip M. Morse and Herman Feshback, Methods of Theoretical Physics, New York: McGraw Hill Book Company, Inc., 1953.

30. Daniel E. Rosner, "Reaction Rates on Partially Blocked Rotating Disk - Effect of Chemical Kinetic Limitations," Journal of the Electrochemical Society, 113 (1966), 624-625.

31. Daniel E. Rosner, "Effects of convective diffusion on the apparent kinetics of zeroth order surface-catalysed chemical reactions," Chemical Engineering Science, 21 (1966), 223-239.

32. B. Levich, "The Theory of Concentration Polarization," Acta Physicochimica U.R.S.S., 17 (1942), 257-307.

33. Heinz Gerischer, "Eine Einführung in die Method zur Untersuchung der Kinetik von Elektrodenprozessen," Zeitschrift für Elektrochemie, 59 (1955), 604-612.

34. Paul Delahay, Double Layer and Electrode Kinetics, New York: Interscience Publishers, 1965, p. 170.

35. Andreas Acrivos and Paul L. Chambré, "Laminar Boundary Layer Flows with Surface Reactions," Industrial and Engineering Chemistry, 49 (1957), 1025-1029.

36. Charles Milton Mohr, Jr., Mass Transfer in Rotating Electrode Systems, Ph.D. Dissertation, University of California, Berkeley, 1975.

37. Limin Hsueh, Diffusion and Migration in Electrochemical Systems, Ph.D. Dissertation, University of California, Berkeley, 1968.

38. John Newman and Limin Hsueh, "Currents Limited by Gas Solubility," Industrial and Engineering Chemistry Fundamentals, 9 (1970), 677-679.

39. O. R. Brown and H. R. Thirsk, "The Rate-Determining Step in the Electrodeposition of Copper on Copper from Aqueous Cupric Sulfate Solutions," Electrochimica Acta, 10 (1965), 383-393.

40. Charles M. Mohr, Jr., and John Newman, "Mass Transfer to a Rotating Disk in Transition Flow," Journal of the Electrochemical Society, 123 (1976), 1687-1691.

41. Leonard Nanis and Wallace Kesselman, "Engineering Applications of Current and Potential Distributions in Disk Electrode Systems," Journal of the Electrochemical Society, 118 (1971), 454-461.

42. Charles K. Bon, Supersaturation at Gas-Evolving Electrodes, M.S. Thesis, University of California, Berkeley, 1970.

43. John Newman, "Resistance for Flow of Current to a Disk," Journal of the Electrochemical Society, 113 (1966), 501-502.

44. Ralph White, Charles M. Mohr, Jr., and John Newman, "The Fluid Motion Due to a Rotating Disk," Journal of the Electrochemical Society, 123 (1976), 383-385.

This report was done with support from the United States Energy Research and Development Administration. Any conclusions or opinions expressed in this report represent solely those of the author(s) and not necessarily those of The Regents of the University of California, the Lawrence Berkeley Laboratory or the United States Energy Research and Development Administration.

TECHNICAL INFORMATION DIVISION
LAWRENCE BERKELEY LABORATORY
UNIVERSITY OF CALIFORNIA
BERKELEY, CALIFORNIA 94720